Research Square

Preprints are preliminary reports that have not undergone peer review.
They should not be considered conclusive, used to inform clinical practice,
or referenced by the media as validated information.

Polarized optical emission reveals a tidal disruption event jet

Alberto Floris

alby.floris@gmail.com

University of Crete https://orcid.org/0009-0004-1671-5454

Ioannis Liodakis

Foundation for Research and Technology https://orcid.org/0000-0001-9200-4006

Karri Koljonen

Norwegian University of Science and Technology https://orcid.org/0000-0002-9677-1533

Kari Nilsson

Finnisi MAGIC Group: Finnish Centre for Astronomy with ESO, University of Turku, FI-20014 Turku

Elina Lindfors

Tuorla Observatory

Odelia Teboul

Weizmann Institute of Science

Alessandro Paggi

Istituto di Radioastronomia

Dmitry Blinov

Institute of Astrophysics - FORTH

Tapio Pursimo

Nordic Optical Telescope

Article

Keywords:

Posted Date: October 9th, 2026

DOI: https://doi.org/10.21203/rs.3.rs-10557323/v1

License: This work is licensed under a Creative Commons Attribution 4.0 International License.
Read Full License

Additional Declarations: There is **NO** Competing Interest.

Polarized optical emission reveals a tidal disruption event jet

Alberto Floris[1,2,3*], Ioannis Liodakis[2,4], Karri I. I. Koljonen[5], Kari Nilsson[7], Elina Lindfors[6,7], Odelia Teboul[8], Alessandro Paggi[9], Dmitriy Blinov[2], Tapio Pursimo[10]

[1]Department of Physics, University of Crete, Voutes University Campus, Vassilika Vouton, 70013, Heraklion, Greece.
[2]Institute of Astrophysics, FORTH, N. Plastira 100, Vassilika Vouton, 70013, Heraklion, Greece.
[3]Osservatorio Astrofisico di Padova, Istituto Nazionale di Astrofisica (INAF), Vicolo dell'osservatorio 5, Padova, 35122, Italy.
[4]Institute of Astrobiology, University of Crete, Voutes University Campus, Vassilika Vouton, 70013, Heraklion, Greece.
[5]Institut for Fysikk, Norwegian University of Science and Technology, Høgskloreringen 5, Trondheim, 7491, Norway.
[6]Department of Physics and Astronomy, University of Turku, Vesillinnantie 5, Turku, 20014, Finland.
[7]Finnish Centre for Astronomy with ESO (FINCA), University of Turku, Vesilinnantie 5, Turku, 20014, Finland.
[8]Department of Particle Physics & Astrophysics, Weizmann Institute of Science, Rehovot, 76100, Israel.
[9]Istituto di Radioastronomia, Istituto Nazionale di Astrofisica (INAF), Via Gobetti 101, Bologna, 40129, Italy.
[10]Nordic Optical Telescope Apartado 474, Santa Cruz de la Palma, 38700, Santa Cruz de Tenerife, Spain.

*Corresponding author(s). E-mail(s): afloris@ia.forth.gr;

Abstract

When a star passes too close to a supermassive black hole (SMBH), it is torn apart and produce a luminous, short-lived accretion episode that reveals a black hole that might otherwise be invisible [1–3]. These tidal disruption events (TDEs)

provide a direct way to observe the onset of accretion around SMBHs in real time, including phases in which the mass accretion rate can be super-Eddington and relativistic, collimated outflows (jets) may be launched [4, 5]. While nearly all confirmed TDEs have been observed at the centers of galaxies, a recent event – AT2024tvd – changed the paradigm. AT2024tvd occurred away from the center of its host galaxy and showed X-ray emission together with two radio flares, indicating continued activity beyond the optical flare [6–8]. The origin of multi-wavelength emission in TDEs is still debated, particularly for delayed radio flares, which may arise from relativistic jets, delayed non-relativistic outflows or shocks driven by outflowing debris interacting with the circumnuclear medium [9, 10]. Here we report optical polarimetric observations of AT2024tvd that provide a missing constraint. Near the optical peak, the intrinsic polarization was modest, while at the peak of the X-ray emission and the onset of the second radio flare, the intrinsic optical polarization reached $\mathbf{\Pi = 24.4^{+7.8}_{-5.9}\%}$. Such high polarization in combination with the multiwavelength behavior points to the presence of a relativistic jet. Our observations suggest that delayed radio rebrightenings in TDEs can mark the emergence of a jet, and demonstrate the power of polarimetry for revealing jet activity that might otherwise remain hidden.

1 Introduction

When a star is disrupted by a SMBH, part of the stellar debris remains bound and can form an accretion flow around the SMBH on timescales of days to months [1, 2, 11]. In TDEs, the early fallback rate is often expected to be super-Eddington, meaning that matter is supplied faster than it can be steadily radiated away by a thin disk [12–14]. In this regime, theory predicts the formation of a geometrically thick flow that can launch powerful winds and, if the magnetic field configuration and black hole spin conditions are favorable, a relativistic jet [4, 12, 15–17]. TDEs therefore offer a direct way to study how jets form in newly fed massive black holes. Powerful relativistic jets have been observed in a small number of TDEs [18–20], but most optically selected events are dominated by optical and ultraviolet emission, even when they later develop X-ray or radio activity [5, 11, 21]. The physical connection between the thermal flare, delayed X-ray emission, radio activity and jet formation therefore remains uncertain.

AT2024tvd is an exceptional event in which to investigate this question because it is unusual in both its location and its time evolution. It was discovered by the Zwicky Transient Facility (ZTF; [22]) and classified spectroscopically as a TDE through its broad hydrogen and helium emission lines [23]. High-resolution imaging later showed that the transient was displaced by 0.808 ± 0.009 kpc in projection from the apparent center of its host galaxy, making it the first confirmed optically selected off-nuclear TDE [6, 24]. Its optical, ultraviolet, and X-ray properties are otherwise broadly consistent with those of nuclear TDEs, including a hot ultraviolet/optical continuum, broad emission lines and delayed soft X-ray emission [6]. The inferred black-hole mass ($\log(M_{\rm BH}/M_\odot) \sim 6.0$; [6, 25]) is substantially lower than expected for the central black hole of the host galaxy ($\log(M_{\rm BH,host}/M_\odot) = 8.37 \pm 0.51$; [6]). This points instead to a displaced massive black hole, possibly due to a past merger or dynamical recoil [6].

Follow-up James Webb Space Telescope (JWST) and W. M. Keck Observatory observations further showed that the transient is associated with excess compact stellar emission at its location, consistent with a massive nuclear star cluster or an ultra-compact dwarf galaxy. This strengthens the interpretation that AT2024tvd is powered by a black hole brought to its present location by a galactic merger [6].

This off-nuclear location opens a direct observational window onto a population of black holes that are otherwise extremely difficult to find. Displaced, wandering or recoiling black holes are hard to identify when they are dormant, because they do not reside at the luminous centers where massive black holes are usually sought [26, 27]. TDEs can temporarily reveal this hidden population by providing a short-lived accretion episode. Other off-nuclear TDE candidates have been identified in X-ray and optical surveys [28–33]. Together with demographic modeling of wandering black holes, these discoveries indicate that off-nuclear TDEs can trace a small but physically important population of massive black holes outside galactic nuclei [25–27, 34].

AT2024tvd is also a laboratory for studying how a newly formed accretion flow evolves. Radio observations showed that the event was radio bright, making it the first confirmed radio-bright off-nuclear TDE [8, 35]. Continued radio and millimeter monitoring revealed a rapidly evolving system, with two radio flares separated in time [8]. In TDEs, radio emission is not expected from the thermal optical photosphere itself; it usually traces synchrotron radiation from fast material interacting with gas around the black hole, where the fast material may be a jet, a broader outflow or shock-powered ejecta [5, 36, 37]. The radio detection therefore shows that the disruption produced additional activity, but by itself does not uniquely determine the precise mechanism producing the emission.

Polarimetry provides an independent way to test this. The polarization of optical light is sensitive to the geometry of the emitting region, to scattering in surrounding material, and to the ordering of magnetic fields. A nearly spherical thermal photosphere is expected to produce little net polarization [38, 39], because different polarization directions cancel out. By contrast, a flattened reprocessing layer, an asymmetric outflow, a shock with partially ordered magnetic fields or synchrotron-emitting material associated with a jet can produce a much larger polarization signal [19, 40]. Polarimetry is therefore especially well suited to AT2024tvd, whose radio and X-ray behavior already suggest that the event departs from the simplest picture of a thermally dominated TDE.

Here we present optical polarimetric observations of AT2024tvd obtained across this critical phase of its evolution. We show that the intrinsic polarization was modest near optical maximum but became remarkably high at a later epoch, contemporaneous with the peak of the X-ray emission [6]. After correcting for dilution by host-galaxy starlight, the B-band polarization reaches a polarization degree of $\Pi = 24.4^{+7.8}_{-5.9}\%$. We argue that this result, together with the radio and X-ray evolution, favors the emergence of a structured jet in which a wide-angle component produces the first delayed radio flare after alignment, while a narrow energetic core becomes visible later through high optical polarization and radio rebrightening [41].

2 Results

Optical polarimetry of AT2024tvd reveals a marked shift in the physics of the emitting region. Near the optical peak, observations with Robopol at the Skinakas 1.3m telescope [42, 43] in the g and r bands show a modest level of intrinsic polarization after correction for dilution by host-galaxy starlight (see the Methods Section for a precise discussion of the adopted techniques). The most constraining measurement at this phase is obtained in the r band, where we measure $\Pi = 4.12 \pm 1.07\%$ at MJD 60599. In the g band we obtain a 3σ upper limit of $\Pi < 4.9\%$. Overall, these measurements are consistent with a weakly to moderately polarized optical source around peak light, as is usually observed in TDEs [44, 45].

The polarization properties changed substantially during the subsequent optical decline. We observed AT2024tvd again with the Alhambra Faint Object Spectrograph and Camera (ALFOSC) mounted on the Nordic Optical Telescope (NOT) at MJD 60710, when the source presented the X-ray peak and the onset of a radio flare [6, 8, 25]. We measure a high intrinsic polarization in the B band, with $\Pi = 24.4^{+7.8}_{-5.9}\%$. Contemporaneous V band observations yielded a 3σ upper limit of $\Pi < 28.6\%$, consistent with the B-band detection. Thus, the strongest polarization is not observed at optical maximum, but instead during the fading phase of the optical light curve, when radio and X-ray emission indicate continued activity from the central engine.

The timing of the polarimetric signal links this change to the broader multiwavelength evolution of the event. Figure 1 shows that the high-polarization epoch occurred after the optical peak, between the two radio flares, and during the phase in which X-ray emission was peaking. At the same time, the X-ray spectrum is better fitted by a blackbody plus a power-law component than by a single thermal component, indicating the emergence of additional non-thermal emission, with this transition from a blackbody spectrum having occurred ~ 70 days after the optical peak [6, 25]. This is the phase in which emission from a delayed jet, if present, is expected to become most visible in the radio and X-ray bands [41].

The measured B-band polarization also constrains the fraction of the optical light that can be thermal. If the observed host-subtracted emission is the sum of a low-polarized, thermal component and a polarized non-thermal component, then a polarization degree as high as $\Pi = 24.4^{+7.8}_{-5.9}\%$ requires a substantial contribution from the latter. Assuming a completely unpolarized thermal component and a maximally polarized ($\Pi_{\rm jet} \simeq 70\%$) synchrotron component for the intrinsic TDE emission, we find a minimum jet contribution of $f_{\rm jet} \simeq 0.35^{+0.11}_{-0.08}$ to the B-band flux. If the thermal component is allowed to be moderately polarized, with $\Pi_{\rm th} \simeq 6\%$ [39] as observed in some TDEs [44, 46, 47], the required minimum contribution from synchrotron/non-thermal emission is $f_{\rm jet} \simeq 0.29^{+0.12}_{-0.09}$. Thus, even under conservative assumptions, at least about one third of the optical light at this epoch must come from a highly polarized component.

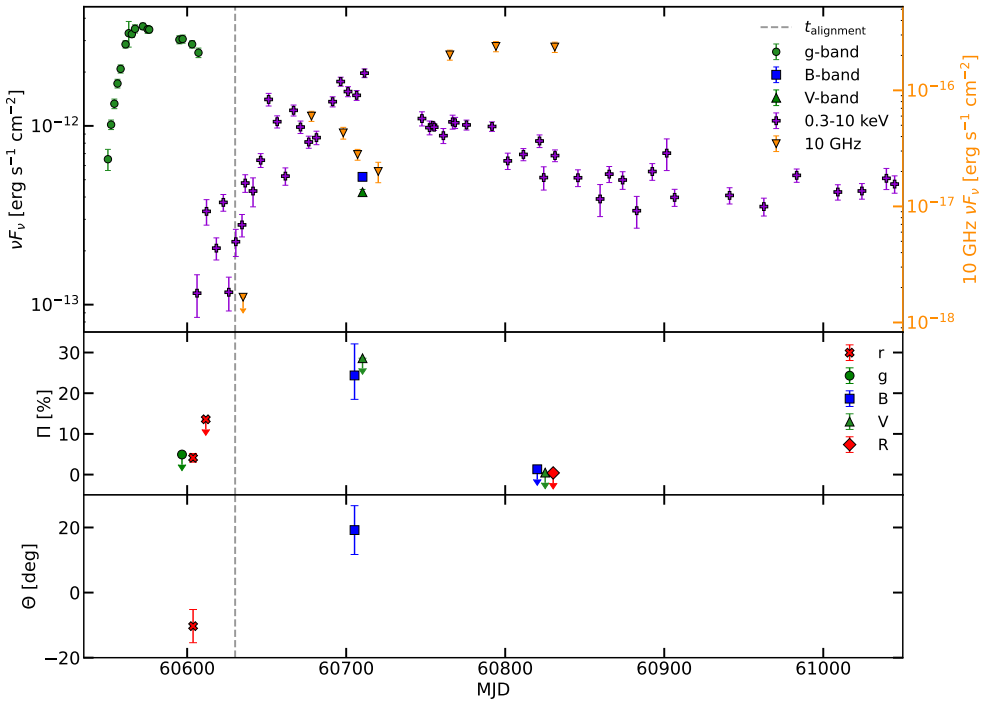


Fig. 1 Optical, X-ray, radio and polarization evolution of AT2024tvd. *Top:* Optical, X-ray and radio light curves. Radio measurements are overlaid on another scale for visual comparison. *Middle:* Multi-band polarization degree measurements. Measurements taken on the same night are horizontally offset by a maximum of 5 days for visual clarity. *Bottom:* Multi-band polarization angle measurements. Non-detections are omitted, as Θ is undefined in such cases. Error bars in the plot identify the 1σ confidence level. The high B-band polarization occurs well after the optical peak, at an epoch contemporaneous with the X-ray peak [6]. The grey dashed line marks the approximate alignment time expected in the delayed jet-breakout interpretation [41].

3 Discussion

The high optical polarization of AT2024tvd provides a direct clue to the mechanism powering the late-time emission. Radio emission in TDEs is usually interpreted as synchrotron radiation from fast material interacting with gas around the black hole. This material may take several forms: a collimated jet, a wider outflow, or shock-powered ejecta launched during the disruption [5, 36, 37, 48, 49]. Distinguishing between these possibilities is difficult, because each can produce delayed radio emission and each can be accompanied by non-thermal radiation [5, 9, 48–50]. AT2024tvd is therefore a particularly useful case. Its radio evolution is not simply delayed, but structured, with two distinct flares [8], and are contemporaneous with the presence of X-ray emission [6] as well as strong optical polarization. A spherical thermal photosphere or an isotropic reprocessing layer cannot explain these features. In such geometries, different polarization directions largely cancel each other when the source is unresolved, leading to a low net polarization [39, 51, 52]. The measured B-band polarization instead requires

that a significant fraction of the optical light arises from some strongly asymmetric structure, and likely from a region in which the magnetic field is at least partially ordered [19, 40, 46, 47]. The polarization alone does not prove that the source is a jet, but it rules out a purely spherical thermal interpretation. Optical polarimetry of other TDEs has also shown that polarized emission can vary with time, indicating that transient asymmetries or shocks can contribute to the observed light [40, 44–47]. In AT2020mot – the only other TDE with a similar reported high polarization degree $\Pi \sim 25\%$ – high polarization detected during the optical decay phase has been interpreted in terms of colliding stellar-stream shocks [40], although no radio or X-ray emission was detected either at early or late times during the evolution of AT2020mot, disfavoring the presence of a jet.

On the contrary, in AT2024tvd the multi-wavelength context favors a jet interpretation. The measured optical polarization is high and temporally associated with the epoch when the X-ray emission peaks and the second radio flare likely begins [6, 8]. At the same time, a successful fit of the X-ray spectrum requires an additional non-thermal component beyond a single blackbody [6, 25]. All of the above are naturally produced by a compact, likely magnetized component whose relative importance grows as the thermal optical flare fades [53–58]. A jet, or a jet-driven shock, provides a direct way to connect these observables within a single physical picture.

Therefore, we interpret the event in the framework of a misaligned, precessing TDE disk-jet system. In this scenario, the orbital angular momentum of the disrupted star is generally misaligned with the SMBH spin axis, so the newly formed accretion disk and any jet launched along the disk's angular momentum axis will also be misaligned [41]. Lense-Thirring torques can then cause the thick disk (and jet) to precess about the SMBH spin axis. Rapid precession, together with super-Eddington disk winds, can inflate a quasi-spherical wind envelope on large scales, and it effectively distributes the jet's power over the precession cone (with characteristic half-opening angle comparable to the misalignment angle), making jet escape more difficult than in the aligned case. As a result, jets with moderate power may be "choked" at early times and only escape once the disk/jet axis has aligned sufficiently with the SMBH spin, producing delayed non-thermal signatures such as late-rising radio emission [41].

For AT2024tvd, the first delayed radio peak and X-ray spectral hardening occur after an inferred alignment/breakout timescale of order 80 days from optical discovery, broadly consistent with the class of delayed/escape scenarios discussed by Teboul and Metzger 41. By analogy with the structured jet picture explored in Teboul and Metzger 41 (e.g., their discussion of pre-alignment wide-angle energy deposition and post-alignment emergence of a narrower core), we associate the first radio peak and X-ray hardening with the emergence of a wider-angle component and the later high optical polarization ($\Delta t \sim 190$ days) and radio rebrightening ($\Delta t \sim 194$ days) with a more compact, energetic component becoming visible once the thermal emission has faded [6, 8, 41]. This sequence provides a simple explanation for why the strongest polarization is not seen at optical maximum but appears later, when the thermal emission has faded and the non-thermal component becomes easier to detect.

Previous polarimetric studies of jetted TDEs provide a useful comparison. The prototype jetted event Swift J1644+57 showed near-infrared linear polarization of

$\Pi \sim 7.4 \pm 3.5\%$ [18]. Swift J2058+0516 showed optical linear polarization of $\Pi \sim 8\%$, interpreted as evidence for a non-thermal contribution to the observed emission [19]. The host-corrected B-band polarization of AT2024tvd is substantially higher than both values. Although the comparison is affected by differences in wavelength, host galaxy dilution and observing phase, it supports the conclusion that the late optical emission of AT2024tvd contains a significant non-thermal component associated with a jet or a jet-driven shock.

The polarization angle (Θ) evolution also supports the emergence of an additional component. The early r-band detection near the optical peak and the later high-polarization B-band epoch have different polarization angles (see Figure 1). A constant foreground interstellar contribution or a constant host-galaxy contribution cannot produce variability in both Π and Θ [45]. Instead, this behavior points to an evolving intrinsically polarized component, as expected if the optical emission becomes increasingly influenced by synchrotron radiation from a jet.

This interpretation also suggests that jet activity in TDEs may be easier to miss than to find. In Swift J1644+57, the relativistic jet faded abruptly as the accretion flow evolved [59]. In misaligned TDE disks, jets may be choked at early times and may escape only after an alignment or breakout phase [41]. AT2024tvd may represent such a transient phase: the polarized component was weak or strongly diluted near optical maximum, but became visible later, once the thermal optical emission had faded and the radio and X-ray signatures of central-engine activity strengthened [6, 8]. If, as we have shown, this phase lasts for only a fraction of the optical light curve, and if the polarized component is further diluted by host-galaxy starlight or residual thermal emission, then many similar jets could remain undetected [44, 45]. Multi-epoch polarimetry, coupled with careful host-galaxy modeling and multi-wavelength observations, may therefore be essential for uncovering a larger population of jet-producing TDEs.

4 Conclusion

Our polarimetric observations show that AT2024tvd developed a highly polarized optical component after correcting for dilution by host galaxy emission. The polarization is too large to be readily produced by a spherical thermal photosphere or an isotropic reprocessing layer [39, 51], and instead implies a strongly asymmetric and likely magnetized emitting region. Combined with the persistent X-ray emission and the double-peaked radio evolution, the observations favor the delayed emergence of a jet after an inferred alignment/breakout timescale of ~ 80 days.

AT2024tvd illustrates two complementary opportunities opened by TDEs. First, TDEs can temporarily illuminate otherwise quiescent massive black holes outside galactic nuclei, providing a way to study the hidden population of displaced or wandering black holes left behind by galaxy mergers [26, 27]. Second, polarimetry can reveal jet activity that may remain ambiguous or missed in photometric and spectroscopic data alone, especially when TDEs occur in bright and nearby galaxies. In this sense, AT2024tvd highlights both the astrophysical importance of off-nuclear TDEs

and the diagnostic power of polarimetry for disentangling the emission mechanisms that power them.

Acknowledgements. AF, IL and AP were funded by the European Union ERC-2022-STG - BOOTES - 101076343. Views and opinions expressed are however those of the author(s) only and do not necessarily reflect those of the European Union or the European Research Council Executive Agency. Neither the European Union nor the granting authority can be held responsible for them. KIIK has received funding from the European Research Council (ERC) under the European Union's Horizon 2020 research and innovation programme (grant agreement No. 101002352, PI: M. Linares).DB acknowledges support from the European Research Council (ERC) under the Horizon ERC Grants 2021 program under grant agreement No. 101040021.The data in this study include observations made with the Nordic Optical Telescope, owned in collaboration by the University of Turku and Aarhus University, and operated jointly by Aarhus University, the University of Turku and the University of Oslo, representing Denmark, Finland and Norway, the University of Iceland and Stockholm University at the Observatorio del Roque de los Muchachos, La Palma, Spain, of the Instituto de Astrofisica de Canarias. The data presented here were obtained in part with ALFOSC, which is provided by the Instituto de Astrofísica de Andalucía (IAA) under a joint agreement with the University of Copenhagen and NOT. This research has made use of data from the RoboPol polarimeter mounted at Skinakas Observatory in Crete, Greece. This work made use of data supplied by the UK Swift Science Data Centre at the University of Leicester.

Corresponding author. Alberto Floris (afloris@ia.forth.gr)

Author contributions. AF performed the analysis and wrote the paper. AF, DB, and IL contributed with the RoboPol observations. EL, KIIK, TP contributed with the NOT observations. AP and KIIK contributed with the multiwavelength data. KN contributed to the host galaxy correction. OT contributed with the theoretical modelling. All the authors contributed to the interpretations of the results and parts of the paper.

Competing interests. Authors declare that they have no competing interests.

Data availability. The reduced polarimetric measurements used in this work are provided in Table 1. The ZTF optical photometry is publicly available through ZTF data services and ALeRCE. Swift/XRT data are publicly available through the Swift archive and the UK Swift Science Data Centre. The radio measurements used for comparison were published by Sfaradi et al. [8] and were accessed through the Open mulTiwavelength Transient Event Repository [60].

References

[1] Hills, J.G.: Possible power source of Seyfert galaxies and QSOs. **254**(5498), 295–298 (1975) https://doi.org/10.1038/254295a0

[2] Rees, M.J.: Tidal disruption of stars by black holes of 10^6-10^8 solar masses in nearby galaxies. **333**(6173), 523–528 (1988) https://doi.org/10.1038/333523a0

[3] Gezari, S., Chornock, R., Rest, A., Huber, M.E., Forster, K., Berger, E., Challis, P.J., Neill, J.D., Martin, D.C., Heckman, T., Lawrence, A., Norman, C., Narayan, G., Foley, R.J., Marion, G.H., Scolnic, D., Chomiuk, L., Soderberg, A., Smith, K., Kirshner, R.P., Riess, A.G., Smartt, S.J., Stubbs, C.W., Tonry, J.L., Wood-Vasey, W.M., Burgett, W.S., Chambers, K.C., Grav, T., Heasley, J.N., Kaiser, N., Kudritzki, R.-P., Magnier, E.A., Morgan, J.S., Price, P.A.: An ultraviolet-optical flare from the tidal disruption of a helium-rich stellar core. **485**(7397), 217–220 (2012) https://doi.org/10.1038/nature10990 arXiv:1205.0252 [astro-ph.CO]

[4] Dai, L., McKinney, J.C., Roth, N., Ramirez-Ruiz, E., Miller, M.C.: A Unified Model for Tidal Disruption Events. **859**(2), 20 (2018) https://doi.org/10.3847/2041-8213/aab429 arXiv:1803.03265 [astro-ph.HE]

[5] Alexander, K.D., van Velzen, S., Horesh, A., Zauderer, B.A.: Radio Properties of Tidal Disruption Events. **216**(5), 81 (2020) https://doi.org/10.1007/s11214-020-00702-w arXiv:2006.01159 [astro-ph.HE]

[6] Yao, Y., Chornock, R., Ward, C., Hammerstein, E., Sfaradi, I., Margutti, R., Kelley, L.Z., Lu, W., Liu, C., Wise, J., Sollerman, J., Alexander, K.D., Bellm, E.C., Drake, A.J., Fremling, C., Gilfanov, M., Graham, M.J., Groom, S.L., Hinds, K.R., Kulkarni, S.R., Miller, A.A., Miller-Jones, J.C.A., Nicholl, M., Perley, D.A., Purdum, J., Ravi, V., Rich, R.M., Rehemtulla, N., Riddle, R., Smith, R., Stein, R., Sunyaev, R., van Velzen, S., Wold, A.: A Massive Black Hole 0.8 kpc from the Host Nucleus Revealed by the Offset Tidal Disruption Event AT2024tvd. **985**(2), 48 (2025) https://doi.org/10.3847/2041-8213/add7de arXiv:2502.17661 [astro-ph.GA]

[7] Patra, K.C., Foley, R.J., Earl, N., Davis, K.W., Ramirez-Ruiz, E., Villar, V.A., Gomez, S., French, K.D., Taggart, K., Arunachalam, P., Macias, P., Kaur, R., Tinyanont, S.: JWST and Keck Observations of the Off-Nuclear TDE AT 2024tvd: A Massive Nuclear Star Cluster and Minor-Merger Origin for its Black Hole. arXiv e-prints, 2510–12572 (2025) https://doi.org/10.48550/arXiv.2510.12572 arXiv:2510.12572 [astro-ph.HE]

[8] Sfaradi, I., Margutti, R., Chornock, R., Alexander, K.D., Metzger, B.D., Beniamini, P., Duran, R.B., Yao, Y., Horesh, A., Farah, W., Berger, E., A. J., N., Cendes, Y., Eftekhari, T., Fender, R., Franz, N., Green, D.A., Hammerstein, E., Lu, W., Wiston, E., Bernstein, Y., Bright, J., Christy, C.T., Cruz, L.F., DeBoer, D.R., Golay, W.W., Goodwin, A.J., Gurwell, M., Keating, G.K., Laskar, T., Miller-Jones, J.C.A., Pollak, A.W., Rao, R., Siemion, A., Sheikh, S.Z., Shoval, N., van Velzen, S.: The First Radio-bright Off-nuclear Tidal Disruption Event AT 2024tvd Reveals the Fastest-evolving Double-peaked Radio Emission. **992**(2), 18 (2025) https://doi.org/10.3847/2041-8213/ae0a26

[9] Horesh, A., Cenko, S.B., Arcavi, I.: Delayed radio flares from a tidal disruption event. Nature Astronomy **5**, 491–497 (2021) https://doi.org/10.1038/s41550-021-01300-8 arXiv:2102.11290 [astro-ph.HE]

[10] Alexander, K.D., Margutti, R., Gomez, S., Stroh, M., Chornock, R., Laskar, T., Cendes, Y., Berger, E., Eftekhari, T., Franz, N., Hajela, A., Metzger, B.D., Terreran, G., Bietenholz, M., Christy, C., De Colle, F., Komossa, S., Nicholl, M., Ramirez-Ruiz, E., Saxton, R., Schroeder, G., Williams, P.K.G., Wu, W.: The Multiwavelength Context of Delayed Radio Emission in Tidal Disruption Events: Evidence for Accretion-driven Outflows. **1000**(1), 139 (2026) https://doi.org/10.3847/1538-4357/ae40ab arXiv:2506.12729 [astro-ph.HE]

[11] Gezari, S.: Tidal Disruption Events. **59**, 21–58 (2021) https://doi.org/10.1146/annurev-astro-111720-030029 arXiv:2104.14580 [astro-ph.HE]

[12] Strubbe, L.E., Quataert, E.: Optical flares from the tidal disruption of stars by massive black holes. **400**, 2070–2084 (2009) https://doi.org/10.1111/j.1365-2966.2009.15599.x arXiv:0905.3735 [astro-ph.CO]

[13] Lodato, G., Rossi, E.M.: Multiband light curves of tidal disruption events. **410**(1), 359–367 (2011) https://doi.org/10.1111/j.1365-2966.2010.17448.x arXiv:1008.4589 [astro-ph.CO]

[14] Guillochon, J., Ramirez-Ruiz, E.: Hydrodynamical Simulations to Determine the Feeding Rate of Black Holes by the Tidal Disruption of Stars: The Importance of the Impact Parameter and Stellar Structure. **767**(1), 25 (2013) https://doi.org/10.1088/0004-637X/767/1/25 arXiv:1206.2350 [astro-ph.HE]

[15] Metzger, B.D., Stone, N.C.: A bright year for tidal disruptions. **461**(1), 948–966 (2016) https://doi.org/10.1093/mnras/stw1394 arXiv:1506.03453 [astro-ph.HE]

[16] Sadowski, A., Narayan, R.: Three-dimensional simulations of supercritical black hole accretion discs - luminosities, photon trapping and variability. **456**(4), 3929–3947 (2016) https://doi.org/10.1093/mnras/stv2941 arXiv:1509.03168 [astro-ph.HE]

[17] Curd, B., Narayan, R.: GRRMHD simulations of tidal disruption event accretion discs around supermassive black holes: jet formation, spectra, and detectability. **483**(1), 565–592 (2019) https://doi.org/10.1093/mnras/sty3134 arXiv:1811.06971 [astro-ph.HE]

[18] Wiersema, K., van der Horst, A.J., Levan, A.J., Tanvir, N.R., Karjalainen, R., Kamble, A., Kouveliotou, C., Metzger, B.D., Russell, D.M., Skillen, I., Starling, R.L.C., Wijers, R.A.M.J.: Polarimetry of the transient relativistic jet of GRB 110328/Swift J164449.3+573451. **421**(3), 1942–1948 (2012) https://doi.org/10.1111/j.1365-2966.2011.20379.x arXiv:1112.3042 [astro-ph.CO]

[19] Wiersema, K., Higgins, A.B., Levan, A.J., Eyles, R.A.J., Starling, R.L.C., Tanvir, N.R., Cenko, S.B., van der Horst, A.J., Gompertz, B.P., Greiner, J., Pasham, D.R.: Polarimetry of relativistic tidal disruption event Swift J2058+0516. **491**(2), 1771–1776 (2020) https://doi.org/10.1093/mnras/stz3106 arXiv:1910.11624 [astro-ph.HE]

[20] Cikota, A., Leloudas, G., Bulla, M., Dai, L., Maund, J., Andreoni, I.: Linear and Circular Polarimetry of the Optically Bright Relativistic Tidal Disruption Event AT 2022cmc. **943**(2), 18 (2023) https://doi.org/10.3847/2041-8213/acaf67 arXiv:2301.00499 [astro-ph.HE]

[21] van Velzen, S., Holoien, T.W.-S., Onori, F., Hung, T., Arcavi, I.: Optical-Ultraviolet Tidal Disruption Events. **216**(8), 124 (2020) https://doi.org/10.1007/s11214-020-00753-z arXiv:2008.05461 [astro-ph.HE]

[22] Bellm, E.C., Kulkarni, S.R., Graham, M.J., Dekany, R., Smith, R.M., Riddle, R., Masci, F.J., Helou, G., Prince, T.A., Adams, S.M., Barbarino, C., Barlow, T., Bauer, J., Beck, R., Belicki, J., Biswas, R., Blagorodnova, N., Bodewits, D., Bolin, B., Brinnel, V., Brooke, T., Bue, B., Bulla, M., Burruss, R., Cenko, S.B., Chang, C.-K., Connolly, A., Coughlin, M., Cromer, J., Cunningham, V., De, K., Delacroix, A., Desai, V., Duev, D.A., Eadie, G., Farnham, T.L., Feeney, M., Feindt, U., Flynn, D., Franckowiak, A., Frederick, S., Fremling, C., Gal-Yam, A., Gezari, S., Giomi, M., Goldstein, D.A., Golkhou, V.Z., Goobar, A., Groom, S., Hacopians, E., Hale, D., Henning, J., Ho, A.Y.Q., Hover, D., Howell, J., Hung, T., Huppenkothen, D., Imel, D., Ip, W.-H., Ivezić, Ž., Jackson, E., Jones, L., Juric, M., Kasliwal, M.M., Kaspi, S., Kaye, S., Kelley, M.S.P., Kowalski, M., Kramer, E., Kupfer, T., Landry, W., Laher, R.R., Lee, C.-D., Lin, H.W., Lin, Z.-Y., Lunnan, R., Giomi, M., Mahabal, A., Mao, P., Miller, A.A., Monkewitz, S., Murphy, P., Ngeow, C.-C., Nordin, J., Nugent, P., Ofek, E., Patterson, M.T., Penprase, B., Porter, M., Rauch, L., Rebbapragada, U., Reiley, D., Rigault, M., Rodriguez, H., van Roestel, J., Rusholme, B., van Santen, J., Schulze, S., Shupe, D.L., Singer, L.P., Soumagnac, M.T., Stein, R., Surace, J., Sollerman, J., Szkody, P., Taddia, F., Terek, S., Van Sistine, A., van Velzen, S., Vestrand, W.T., Walters, R., Ward, C., Ye, Q.-Z., Yu, P.-C., Yan, L., Zolkower, J.: The Zwicky Transient Facility: System Overview, Performance, and First Results. **131**(995), 018002 (2019) https://doi.org/10.1088/1538-3873/aaecbe arXiv:1902.01932 [astro-ph.IM]

[23] Faris, S., Arcavi, I., Newsome, M., Farah, J., Andrews, M., Howell, D.A., McCully, C.: StarDestroyers Transient Classification Report for 2024-10-14. Transient Name Server Classification Report **2024-4005**, 1 (2024)

[24] Yao, Y., Chornock, R., Margutti, R., Ward, C., Sfaradi, I., Hammerstein, E., Stein, R.: AT2024tvd: an off-nuclear tidal disruption event. Transient Name Server AstroNote **13**, 1 (2025)

[25] Guolo, M., Mummery, A., van Velzen, S., Nicholl, M., Gezari, S., Yao, Y.,

Chambers, K.C., de Boer, T., Huber, M.E., Lin, C.-C., Lowe, T.B., Magnier, E.A., Paek, G., Wainscoat, R.: The Wandering Supermassive Black Hole Powering the off-nuclear TDE AT2024tvd. arXiv e-prints, 2602–12272 (2026) https://doi.org/10.48550/arXiv.2602.12272 arXiv:2602.12272 [astro-ph.HE]

[26] Blecha, L., Sijacki, D., Kelley, L.Z., Torrey, P., Vogelsberger, M., Nelson, D., Springel, V., Snyder, G., Hernquist, L.: Recoiling black holes: prospects for detection and implications of spin alignment. **456**(1), 961–989 (2016) https://doi.org/10.1093/mnras/stv2646 arXiv:1508.01524 [astro-ph.GA]

[27] Volonteri, M., Habouzit, M., Colpi, M.: The origins of massive black holes. Nature Reviews Physics **3**(11), 732–743 (2021) https://doi.org/10.1038/s42254-021-00364-9 arXiv:2110.10175 [astro-ph.GA]

[28] Lin, D., Strader, J., Carrasco, E.R., Page, D., Romanowsky, A.J., Homan, J., Irwin, J.A., Remillard, R.A., Godet, O., Webb, N.A., Baumgardt, H., Wijnands, R., Barret, D., Duc, P.-A., Brodie, J.P., Gwyn, S.D.J.: A luminous X-ray outburst from an intermediate-mass black hole in an off-centre star cluster. Nature Astronomy **2**, 656–661 (2018) https://doi.org/10.1038/s41550-018-0493-1 arXiv:1806.05692 [astro-ph.HE]

[29] Lin, D., Strader, J., Romanowsky, A.J., Irwin, J.A., Godet, O., Barret, D., Webb, N.A., Homan, J., Remillard, R.A.: Multiwavelength Follow-up of the Hyperluminous Intermediate-mass Black Hole Candidate 3XMM J215022.4-055108. **892**(2), 25 (2020) https://doi.org/10.3847/2041-8213/ab745b arXiv:2002.04618 [astro-ph.HE]

[30] Jin, C.-C., Li, D.-Y., Jiang, N., Dai, L.-X., Cheng, H.-Q., Zhu, J.-Z., Yang, C.-W., Rau, A., Baldini, P., Wang, T.-G., Zhou, H.-Y., Yuan, W., Zhang, C., Shu, X.-W., Shen, R.-F., Wang, Y.-L., Wen, S.-X., Wu, Q.-Y., Wang, Y.-B., Thomsen, L.L., Zhang, Z.-J., Zhang, W.-J., Coleiro, A., Eyles-Ferris, R., Fang, X., Ho, L.C., Hu, J.-W., Jin, J.-J., Li, W.-X., Liu, B.-F., Liu, F.-K., Liu, M.-J., Liu, Z., Lu, Y.-J., Merloni, A., Qiao, E.-L., Saxton, R., Soria, R., Wang, S., Xue, Y.-Q., Yang, H.-N., Zhang, B., Zhang, W.-D., Cai, Z.-M., Chen, F.-S., Chen, H.-L., Chen, T.-X., Chen, W., Chen, Y.-H., Chen, Y.-F., Chen, Y., Cordier, B., Cui, C.-Z., Cui, W.-W., Dai, Y.-F., Ding, H.-C., Fan, D.-W., Fan, Z., Feng, H., Garcia, J.A., Guan, J., Han, D.-W., Hou, D.-J., Hu, H.-B., Huang, M.-H., Huo, J., Jia, S.-M., Jia, Z.-Q., Jiang, B.-W., Jin, G., Kong, X., Kuulkers, E., Lei, W.-H., Li, C.-K., Li, J.-F., Li, L.-H., Li, M.-S., Li, W., Li, Z.-D., Lian, T.-Y., Ling, Z.-X., Liu, C.-Z., Liu, H.-Y., Liu, H.-Q., Liu, J.-F., Liu, Y., Lu, F.-J., Luo, L.-D., Ma, J., Mao, X., Mu, H.-Y., Nandra, K., O'Brien, P., Pan, H.-W., Pan, X., Qin, G.-J., Rea, N., Sanders, J., Song, L.-M., Sun, H., Sun, S.-L., Sun, X.-J., Tan, Y.-Y., Tang, Q.-J., Tao, Y.-H., Wang, B.-C., Wang, J., Wang, J.-F., Wang, L., Wang, W.-X., Wang, Y.-S., Wang, Z.-X., Wu, Q.-W., Wu, X.-F., Xu, H.-T., Xu, J.-J., Xu, X.-P., Xu, Y.-F., Xu, Z., Xue, C.-B., Xue, S.-J., Xue, Y.-L., Yan, A.-L., Yang, X.-T., Yang, Y.-J., Zhang, J., Zhang, M., Zhang, S.-N., Zhang, Y.-H., Zhang, Z., Zhang, Z., Zhang,

Z.-L., Zhao, D.-H., Zhao, H.-S., Zhao, X.-F., Zhao, Z.-J., Zheng, J., Zhu, Q.-F., Zhu, Y.-X., Zhu, Z.-C., Zou, H.: An Intermediate-mass Black Hole Lurking in A Galactic Halo Caught Alive during Outburst. arXiv e-prints, 2501–09580 (2025) https://doi.org/10.48550/arXiv.2501.09580 arXiv:2501.09580 [astro-ph.HE]

[31] Stein, R., Carney, J., Ward, C., Margutti, R., Hall, X.J., Sfaradi, I., Andreoni, I., Chornock, R., Gezari, S., Mo, G., Yao, Y., Bellm, E.C., Bloom, J.S., Busmann, M., Caiazzo, I., Cenko, S.B., Graham, M.J., Groom, S.L., Gruen, D., Hammerstein, E., Kasliwal, M.M., O'Connor, B., Palmese, A., Purdum, J., Rastinejad, J.C., Riddle, R., Rusholme, B., Sollerman, J., Somalwar, J.J., Veilleux, S.: TDE 2025abcr: A Tidal Disruption Event in the Outskirts of a Massive Galaxy. arXiv e-prints, 2602–10180 (2026) https://doi.org/10.48550/arXiv.2602.10180 arXiv:2602.10180 [astro-ph.HE]

[32] Patra, K.C., Liepold, E.R., Earl, N., Foley, R.J., Ma, C.-P., Gomez, S., Davis, K.W., Ramirez-Ruiz, E., French, K.D., Walsh, J.L., Kaur, R., Taggart, K., Candanoza, J., Villar, V.A., Arunachalam, P., Macias, P., Tinyanont, S.: JWST and Keck observations of the off-nuclear tidal disruption event TDE 2025abcr: An evolving reprocessing layer. arXiv e-prints, 2604–16093 (2026) arXiv:2604.16093 [astro-ph.HE]

[33] Li, W., Christy, C.T., Alexander, K.D., Sfaradi, I., Huang, X., Jiang, N., Laskar, T., Mummery, A., Franz, N., Goodwin, A.J., Golay, W.W., Margutti, R., Chornock, R., Zhu, J., van Velzen, S., Cendes, Y., Lu, W., Lynch, J.: VLA Observations Confirm AT 2023mfm as an Off-nuclear Tidal Disruption Event. arXiv e-prints, 2606–06595 (2026) https://doi.org/10.48550/arXiv.2606.06595 arXiv:2606.06595 [astro-ph.HE]

[34] Guolo, M.: Demographics of Wandering Black Holes Powering Off-Nuclear Tidal Disruption Events. arXiv e-prints, 2602–12970 (2026) https://doi.org/10.48550/arXiv.2602.12970 arXiv:2602.12970 [astro-ph.GA]

[35] Sfaradi, I., Chornock, R., Alexander, K.D., Margutti, R., Yao, Y., Nayana, A.J., Berger, E., Cendes, Y., Christy, C.T., Eftekhari, T., Franz, N., Golay, W.W., Gomez, S., Goodwin, A.J., Hammerstein, E., Ramirez-Ruiz, E.: VLA radio detection of the off-nuclear TDE AT 2024tvd. Transient Name Server AstroNote **14**, 1 (2025)

[36] Giannios, D., Metzger, B.D.: Radio transients from stellar tidal disruption by massive black holes. **416**(3), 2102–2107 (2011) https://doi.org/10.1111/j.1365-2966.2011.19188.x arXiv:1102.1429 [astro-ph.HE]

[37] De Colle, F., Lu, W.: Jets from Tidal Disruption Events. **89**, 101538 (2020) https://doi.org/10.1016/j.newar.2020.101538 arXiv:1911.01442 [astro-ph.HE]

[38] Patra, K.C., Lu, W., Brink, T.G., Yang, Y., Filippenko, A.V., Vasylyev, S.S.: Spectropolarimetry of the tidal disruption event AT 2019qiz: a quasi-spherical

reprocessing layer. **515**(1), 138–145 (2022) https://doi.org/10.1093/mnras/stac1727 arXiv:2206.09039 [astro-ph.HE]

[39] Leloudas, G., Bulla, M., Cikota, A., Dai, L., Thomsen, L.L., Maund, J.R., Charalampopoulos, P., Roth, N., Arcavi, I., Auchettl, K., Malesani, D.B., Nicholl, M., Ramirez-Ruiz, E.: An asymmetric electron-scattering photosphere around optical tidal disruption events. Nature Astronomy **6**, 1193–1202 (2022) https://doi.org/10.1038/s41550-022-01767-z arXiv:2207.06855 [astro-ph.HE]

[40] Liodakis, I., Koljonen, K.I.I., Blinov, D., Lindfors, E., Alexander, K.D., Hovatta, T., Berton, M., Hajela, A., Jormanainen, J., Kouroumpatzakis, K., Mandarakas, N., Nilsson, K.: Optical polarization from colliding stellar stream shocks in a tidal disruption event. Science **380**(6645), 656–658 (2023) https://doi.org/10.1126/science.abj9570 arXiv:2208.14465 [astro-ph.HE]

[41] Teboul, O., Metzger, B.D.: A Unified Theory of Jetted Tidal Disruption Events: From Promptly Escaping Relativistic to Delayed Transrelativistic Jets. **957**(1), 9 (2023) https://doi.org/10.3847/2041-8213/ad0037 arXiv:2308.05161 [astro-ph.HE]

[42] King, O.G., Blinov, D., Ramaprakash, A.N., Myserlis, I., Angelakis, E., Baloković, M., Feiler, R., Fuhrmann, L., Hovatta, T., Khodade, P., Kougentakis, A., Kylafis, N., Kus, A., Modi, D., Paleologou, E., Panopoulou, G., Papadakis, I., Papamastorakis, I., Paterakis, G., Pavlidou, V., Pazderska, B., Pazderski, E., Pearson, T.J., Rajarshi, C., Readhead, A.C.S., Reig, P., Steiakaki, A., Tassis, K., Zensus, J.A.: The RoboPol pipeline and control system. **442**(2), 1706–1717 (2014) https://doi.org/10.1093/mnras/stu176 arXiv:1310.7555 [astro-ph.IM]

[43] Ramaprakash, A.N., Rajarshi, C.V., Das, H.K., Khodade, P., Modi, D., Panopoulou, G., Maharana, S., Blinov, D., Angelakis, E., Casadio, C., Fuhrmann, L., Hovatta, T., Kiehlmann, S., King, O.G., Kylafis, N., Kougentakis, A., Kus, A., Mahabal, A., Marecki, A., Myserlis, I., Paterakis, G., Paleologou, E., Liodakis, I., Papadakis, I., Papamastorakis, I., Pavlidou, V., Pazderski, E., Pearson, T.J., Readhead, A.C.S., Reig, P., Słowikowska, A., Tassis, K., Zensus, J.A.: RoboPol: a four-channel optical imaging polarimeter. **485**(2), 2355–2366 (2019) https://doi.org/10.1093/mnras/stz557 arXiv:1902.08367 [astro-ph.IM]

[44] Floris, A., Liodakis, I., Koljonen, K.I.I., Lindfors, E., Agís-Gonzalez, B., Paggi, A., Blinov, D., Nilsson, K., Agudo, I., Charalampopoulos, P., Díaz Teodori, M.A., Escudero Pedrosa, J., Otero-Santos, J., Piirola, V., Newsome, M., Van Velzen, S.: Polarimetric diversity in tidal disruption events: Comparative study of low-polarised sources with AT2020mot. **703**, 81 (2025) https://doi.org/10.1051/0004-6361/202555626 arXiv:2509.08895 [astro-ph.HE]

[45] Floris, A., Liodakis, I., Koljonen, K.I.I., Lindfors, E., Agís-González, B., Paggi, A., Blinov, D., Nilsson, K., Agudo, I., Charalampopoulos, P., Escudero Pedrosa, J., Piirola, V.: Polarisation angle variability in tidal disruption events. **707**, 378

(2026) https://doi.org/10.1051/0004-6361/202557658 arXiv:2603.02324 [astro-ph.HE]

[46] Koljonen, K.I.I., Liodakis, I., Lindfors, E., Nilsson, K., Reynolds, T.M., Charalampopoulos, P., Kouroumpatzakis, K., McCall, C., Jermak, H.E., Steele, I.A., Carbajo-Hijarrubia, J.: The extreme coronal line emitter AT 2022fpx: varying optical polarization properties and late-time X-ray flare. **532**(1), 112–125 (2024) https://doi.org/10.1093/mnras/stae1466 arXiv:2403.04877 [astro-ph.HE]

[47] Koljonen, K.I.I., Nilsson, K., Liodakis, I., Lindfors, E.: Optical polarization properties of the closest tidal disruption event AT 2023clx indicate origin from tidal stream shocks. **542**(3), 2238–2244 (2025) https://doi.org/10.1093/mnras/staf1340 arXiv:2508.09309 [astro-ph.HE]

[48] Goodwin, A.J., Miller-Jones, J.C.A., van Velzen, S., Bietenholz, M., Greenland, J., Cenko, B., Gezari, S., Horesh, A., Sivakoff, G.R., Yan, L., Yu, W., Zhang, X.: Radio observations of the tidal disruption event AT2020opy: a luminous non-relativistic outflow encountering a dense circumnuclear medium. **518**(1), 847–854 (2023) https://doi.org/10.1093/mnras/stac3127 arXiv:2208.13967 [astro-ph.HE]

[49] Cendes, Y., Berger, E., Alexander, K.D., Chornock, R., Margutti, R., Metzger, B., Wieringa, M.H., Bietenholz, M.F., Hajela, A., Laskar, T., Stroh, M.C., Terreran, G.: Ubiquitous Late Radio Emission from Tidal Disruption Events. **971**(2), 185 (2024) https://doi.org/10.3847/1538-4357/ad5541 arXiv:2308.13595 [astro-ph.HE]

[50] Horesh, A., Sfaradi, I., Fender, R., Green, D.A., Williams, D.R.A., Bright, J.S.: Are Delayed Radio Flares Common in Tidal Disruption Events? The Case of the TDE iPTF 16fnl. **920**(1), 5 (2021) https://doi.org/10.3847/2041-8213/ac25fe arXiv:2109.10921 [astro-ph.HE]

[51] Chandrasekhar, S.: Radiative Transfer, (1960)

[52] Charalampopoulos, P., Bulla, M., Bonnerot, C., Leloudas, G.: Modeling continuum polarization levels of tidal disruption events based on the collision-induced outflow model. **670**, 150 (2023) https://doi.org/10.1051/0004-6361/202245014 arXiv:2212.05079 [astro-ph.HE]

[53] Burrows, D.N., Kennea, J.A., Ghisellini, G., Mangano, V., Zhang, B., Page, K.L., Eracleous, M., Romano, P., Sakamoto, T., Falcone, A.D., Osborne, J.P., Campana, S., Beardmore, A.P., Breeveld, A.A., Chester, M.M., Corbet, R., Covino, S., Cummings, J.R., D'Avanzo, P., D'Elia, V., Esposito, P., Evans, P.A., Fugazza, D., Gelbord, J.M., Hiroi, K., Holland, S.T., Huang, K.Y., Im, M., Israel, G., Jeon, Y., Jeon, Y.-B., Jun, H.D., Kawai, N., Kim, J.H., Krimm, H.A., Marshall, F.E., P. Mészáros, Negoro, H., Omodei, N., Park, W.-K., Perkins, J.S., Sugizaki, M., Sung, H.-I., Tagliaferri, G., Troja, E., Ueda, Y., Urata, Y., Usui, R., Antonelli, L.A., Barthelmy, S.D., Cusumano, G., Giommi, P., Melandri, A., Perri, M., Racusin,

J.L., Sbarufatti, B., Siegel, M.H., Gehrels, N.: Relativistic jet activity from the tidal disruption of a star by a massive black hole. **476**(7361), 421–424 (2011) https://doi.org/10.1038/nature10374 arXiv:1104.4787 [astro-ph.HE]

[54] Bloom, J.S., Giannios, D., Metzger, B.D., Cenko, S.B., Perley, D.A., Butler, N.R., Tanvir, N.R., Levan, A.J., O'Brien, P.T., Strubbe, L.E., De Colle, F., Ramirez-Ruiz, E., Lee, W.H., Nayakshin, S., Quataert, E., King, A.R., Cucchiara, A., Guillochon, J., Bower, G.C., Fruchter, A.S., Morgan, A.N., van der Horst, A.J.: A Possible Relativistic Jetted Outburst from a Massive Black Hole Fed by a Tidally Disrupted Star. Science **333**(6039), 203 (2011) https://doi.org/10.1126/science.1207150 arXiv:1104.3257 [astro-ph.HE]

[55] Zauderer, B.A., Berger, E., Soderberg, A.M., Loeb, A., Narayan, R., Frail, D.A., Petitpas, G.R., Brunthaler, A., Chornock, R., Carpenter, J.M., Pooley, G.G., Mooley, K., Kulkarni, S.R., Margutti, R., Fox, D.B., Nakar, E., Patel, N.A., Volgenau, N.H., Culverhouse, T.L., Bietenholz, M.F., Rupen, M.P., Max-Moerbeck, W., Readhead, A.C.S., Richards, J., Shepherd, M., Storm, S., Hull, C.L.H.: Birth of a relativistic outflow in the unusual γ-ray transient Swift J164449.3+573451. **476**(7361), 425–428 (2011) https://doi.org/10.1038/nature10366 arXiv:1106.3568 [astro-ph.HE]

[56] Metzger, B.D., Giannios, D., Mimica, P.: Afterglow model for the radio emission from the jetted tidal disruption candidate Swift J1644+57. **420**(4), 3528–3537 (2012) https://doi.org/10.1111/j.1365-2966.2011.20273.x arXiv:1110.1111 [astro-ph.HE]

[57] Andreoni, I., Coughlin, M.W., Perley, D.A., Yao, Y., Lu, W., Cenko, S.B., Kumar, H., Anand, S., Ho, A.Y.Q., Kasliwal, M.M., de Ugarte Postigo, A., Sagués-Carracedo, A., Schulze, S., Kann, D.A., Kulkarni, S.R., Sollerman, J., Tanvir, N., Rest, A., Izzo, L., Somalwar, J.J., Kaplan, D.L., Ahumada, T., Anupama, G.C., Auchettl, K., Barway, S., Bellm, E.C., Bhalerao, V., Bloom, J.S., Bremer, M., Bulla, M., Burns, E., Campana, S., Chandra, P., Charalampopoulos, P., Cooke, J., D'Elia, V., Das, K.K., Dobie, D., Agüí Fernández, J.F., Freeburn, J., Fremling, C., Gezari, S., Goode, S., Graham, M.J., Hammerstein, E., Karambelkar, V.R., Kilpatrick, C.D., Kool, E.C., Krips, M., Laher, R.R., Leloudas, G., Levan, A., Lundquist, M.J., Mahabal, A.A., Medford, M.S., Miller, M.C., Möller, A., Mooley, K.P., Nayana, A.J., Nir, G., Pang, P.T.H., Paraskeva, E., Perley, R.A., Petitpas, G., Pursiainen, M., Ravi, V., Ridden-Harper, R., Riddle, R., Rigault, M., Rodriguez, A.C., Rusholme, B., Sharma, Y., Smith, I.A., Stein, R.D., Thöne, C., Tohuvavohu, A., Valdes, F., van Roestel, J., Vergani, S.D., Wang, Q., Zhang, J.: A very luminous jet from the disruption of a star by a massive black hole. **612**(7940), 430–434 (2022) https://doi.org/10.1038/s41586-022-05465-8 arXiv:2211.16530 [astro-ph.HE]

[58] Pasham, D.R., Lucchini, M., Laskar, T., Gompertz, B.P., Srivastav, S., Nicholl, M., Smartt, S.J., Miller-Jones, J.C.A., Alexander, K.D., Fender, R., Smith, G.P.,

Fulton, M., Dewangan, G., Gendreau, K., Coughlin, E.R., Rhodes, L., Horesh, A., van Velzen, S., Sfaradi, I., Guolo, M., Castro Segura, N., Aamer, A., Anderson, J.P., Arcavi, I., Brennan, S.J., Chambers, K., Charalampopoulos, P., Chen, T.-W., Clocchiatti, A., de Boer, T., Dennefeld, M., Ferrara, E., Galbany, L., Gao, H., Gillanders, J.H., Goodwin, A., Gromadzki, M., Huber, M., Jonker, P.G., Joshi, M., Kara, E., Killestein, T.L., Kosec, P., Kocevski, D., Leloudas, G., Lin, C.-C., Margutti, R., Mattila, S., Moore, T., Müller-Bravo, T., Ngeow, C.-C., Oates, S., Onori, F., Pan, Y.-C., Perez-Torres, M., Rani, P., Remillard, R., Ridley, E.J., Schulze, S., Sheng, X., Shingles, L., Smith, K.W., Steiner, J.F., Wainscoat, R., Wevers, T., Yang, S.: The Birth of a Relativistic Jet Following the Disruption of a Star by a Cosmological Black Hole. Nature Astronomy **7**, 88–104 (2023) https://doi.org/10.1038/s41550-022-01820-x arXiv:2211.16537 [astro-ph.HE]

[59] Levan, A.J., Tanvir, N.R., Brown, G.C., Metzger, B.D., Page, K.L., Cenko, S.B., O'Brien, P.T., Lyman, J.D., Wiersema, K., Stanway, E.R., Fruchter, A.S., Perley, D.A., Bloom, J.S.: Late Time Multi-wavelength Observations of Swift J1644+5734: A Luminous Optical/IR Bump and Quiescent X-Ray Emission. **819**(1), 51 (2016) https://doi.org/10.3847/0004-637X/819/1/51 arXiv:1509.08945 [astro-ph.HE]

[60] Franz, N., Alexander, K.D., Gomez, S., Christy, C.T., Laskar, T., van Velzen, S., Earl, N., Gezari, S., Karmen, M., Margutti, R., Pearson, J., Villar, V.A., Zabludoff, A.I.: The Open mulTiwavelength Transient Event Repository (OTTER): Infrastructure Release and Tidal Disruption Event Catalog. **999**(2), 243 (2026) https://doi.org/10.3847/1538-4357/ae346e arXiv:2509.05405 [astro-ph.HE]

[61] Blinov, D., Kiehlmann, S., Pavlidou, V., Panopoulou, G.V., Skalidis, R., Angelakis, E., Casadio, C., Einoder, E.N., Hovatta, T., Kokolakis, K., Kougentakis, A., Kus, A., Kylafis, N., Kyritsis, E., Lalakos, A., Liodakis, I., Maharana, S., Makrydopoulou, E., Mandarakas, N., Maragkakis, G.M., Myserlis, I., Papadakis, I., Paterakis, G., Pearson, T.J., Ramaprakash, A.N., Readhead, A.C.S., Reig, P., Słowikowska, A., Tassis, K., Xexakis, K., Żejmo, M., Zensus, J.A.: RoboPol: AGN polarimetric monitoring data. **501**(3), 3715–3726 (2021) https://doi.org/10.1093/mnras/staa3777 arXiv:2012.00008 [astro-ph.HE]

[62] Hovatta, T., Lindfors, E., Blinov, D., Pavlidou, V., Nilsson, K., Kiehlmann, S., Angelakis, E., Fallah Ramazani, V., Liodakis, I., Myserlis, I., Panopoulou, G.V., Pursimo, T.: Optical polarization of high-energy BL Lacertae objects. **596**, 78 (2016) https://doi.org/10.1051/0004-6361/201628974 arXiv:1608.08440 [astro-ph.HE]

[63] Andruchow, I., Cellone, S.A., Romero, G.E.: Incidence of the host galaxy on the measured optical linear polarization of blazars. **388**(4), 1766–1774 (2008) https://doi.org/10.1111/j.1365-2966.2008.13502.x arXiv:0805.4421 [astro-ph]

[64] Sersic, J.L.: Atlas de Galaxias Australes, (1968)

[65] Graham, A.W., Driver, S.P.: A Concise Reference to (Projected) Sérsic $R^{1/n}$ Quantities, Including Concentration, Profile Slopes, Petrosian Indices, and Kron Magnitudes. **22**(2), 118–127 (2005) https://doi.org/10.1071/AS05001 arXiv:astro-ph/0503176 [astro-ph]

[66] Flewelling, H.A., Magnier, E.A., Chambers, K.C., Heasley, J.N., Holmberg, C., Huber, M.E., Sweeney, W., Waters, C.Z., Calamida, A., Casertano, S., Chen, X., Farrow, D., Hasinger, G., Henderson, R., Long, K.S., Metcalfe, N., Narayan, G., Nieto-Santisteban, M.A., Norberg, P., Rest, A., Saglia, R.P., Szalay, A., Thakar, A.R., Tonry, J.L., Valenti, J., Werner, S., White, R., Denneau, L., Draper, P.W., Hodapp, K.W., Jedicke, R., Kaiser, N., Kudritzki, R.P., Price, P.A., Wainscoat, R.J., Chastel, S., McLean, B., Postman, M., Shiao, B.: The Pan-STARRS1 Database and Data Products. **251**(1), 7 (2020) https://doi.org/10.3847/1538-4365/abb82d arXiv:1612.05243 [astro-ph.IM]

[67] Tonry, J.L., Stubbs, C.W., Lykke, K.R., Doherty, P., Shivvers, I.S., Burgett, W.S., Chambers, K.C., Hodapp, K.W., Kaiser, N., Kudritzki, R.-P., Magnier, E.A., Morgan, J.S., Price, P.A., Wainscoat, R.J.: The Pan-STARRS1 Photometric System. **750**(2), 99 (2012) https://doi.org/10.1088/0004-637X/750/2/99 arXiv:1203.0297 [astro-ph.IM]

[68] Serkowski, K., Mathewson, D.S., Ford, V.L.: Wavelength dependence of interstellar polarization and ratio of total to selective extinction. **196**, 261–290 (1975) https://doi.org/10.1086/153410

[69] Schlafly, E.F., Finkbeiner, D.P.: Measuring Reddening with Sloan Digital Sky Survey Stellar Spectra and Recalibrating SFD. **737**(2), 103 (2011) https://doi.org/10.1088/0004-637X/737/2/103 arXiv:1012.4804 [astro-ph.GA]

[70] Förster, F., Cabrera-Vives, G., Castillo-Navarrete, E., Estévez, P.A., Sánchez-Sáez, P., Arredondo, J., Bauer, F.E., Carrasco-Davis, R., Catelan, M., Elorrieta, F., Eyheramendy, S., Huijse, P., Pignata, G., Reyes, E., Reyes, I., Rodríguez-Mancini, D., Ruz-Mieres, D., Valenzuela, C., Álvarez-Maldonado, I., Astorga, N., Borissova, J., Clocchiatti, A., De Cicco, D., Donoso-Oliva, C., Hernández-García, L., Graham, M.J., Jordán, A., Kurtev, R., Mahabal, A., Maureira, J.C., Muñoz-Arancibia, A., Molina-Ferreiro, R., Moya, A., Palma, W., Pérez-Carrasco, M., Protopapas, P., Romero, M., Sabatini-Gacitua, L., Sánchez, A., San Martín, J., Sepúlveda-Cobo, C., Vera, E., Vergara, J.R.: The Automatic Learning for the Rapid Classification of Events (ALeRCE) Alert Broker. **161**(5), 242 (2021) https://doi.org/10.3847/1538-3881/abe9bc arXiv:2008.03303 [astro-ph.IM]

[71] Burrows, D.N., Hill, J.E., Nousek, J.A., Kennea, J.A., Wells, A., Osborne, J.P., Abbey, A.F., Beardmore, A., Mukerjee, K., Short, A.D.T., Chincarini, G., Campana, S., Citterio, O., Moretti, A., Pagani, C., Tagliaferri, G., Giommi, P., Capalbi, M., Tamburelli, F., Angelini, L., Cusumano, G., Bräuninger, H.W.,

Burkert, W., Hartner, G.D.: The Swift X-Ray Telescope. **120**(3-4), 165–195 (2005) https://doi.org/10.1007/s11214-005-5097-2 arXiv:astro-ph/0508071 [astro-ph]

[72] Evans, P.A., Beardmore, A.P., Page, K.L., Osborne, J.P., O'Brien, P.T., Willingale, R., Starling, R.L.C., Burrows, D.N., Godet, O., Vetere, L., Racusin, J., Goad, M.R., Wiersema, K., Angelini, L., Capalbi, M., Chincarini, G., Gehrels, N., Kennea, J.A., Margutti, R., Morris, D.C., Mountford, C.J., Pagani, C., Perri, M., Romano, P., Tanvir, N.: Methods and results of an automatic analysis of a complete sample of Swift-XRT observations of GRBs. **397**(3), 1177–1201 (2009) https://doi.org/10.1111/j.1365-2966.2009.14913.x arXiv:0812.3662 [astro-ph]

[73] Houck, J.C.: ISIS: The Interactive Spectral Interpretation System. In: Branduardi-Raymont, G. (ed.) High Resolution X-ray Spectroscopy with XMM-Newton and Chandra, p. 17 (2002)

[74] Wilms, J., Allen, A., McCray, R.: On the Absorption of X-Rays in the Interstellar Medium. **542**(2), 914–924 (2000) https://doi.org/10.1086/317016 arXiv:astro-ph/0008425 [astro-ph]

[75] Stone, N., Loeb, A.: Observing Lense-Thirring Precession in Tidal Disruption Flares. **108**(6), 061302 (2012) https://doi.org/10.1103/PhysRevLett.108.061302 arXiv:1109.6660 [astro-ph.HE]

[76] Chevalier, R.A., Li, Z.-Y.: Wind Interaction Models for Gamma-Ray Burst Afterglows: The Case for Two Types of Progenitors. **536**(1), 195–212 (2000) https://doi.org/10.1086/308914 arXiv:astro-ph/9908272 [astro-ph]

Methods

Optical polarization observations

We obtained optical polarization observations of AT2024tvd close to the peak of the optical emission using the RoboPol polarimeter on the 1.3m Skinakas Observatory telescope. The observations were obtained in the g- and r- bands on MJD 60599 and in the r- band on MJD 60607. The data were reduced using the standard RoboPol pipeline [42, 61], which measures the normalized Stokes parameters q and u from the relative fluxes of the ordinary and extraordinary beams produced by the instrument. We observed AT2024tvd again on MJD 60710 in the B-, V- and R bands with the Alhambra Faint Object Spectrograph and Camera (ALFOSC) mounted on the NOT. The data were reduced using the semi-automatic pipeline for NOT polarimetric data [62], which was previously employed for other TDE studies [44–47], and originally found $\Pi < 0.5\%$ in the B and V bands. The R-band observation was obtained very close to sunrise and was excluded from the transient analysis because the increasing sky brightness produced unreliable background subtraction. We also obtained NOT observations of the host galaxy on MJD 60825, when the transient contribution was

Table 1 Polarimetric measurements of AT2024tvd

MJD [d] (1)	$\Delta t_{\rm peak}$ [d] (2)	Π [%] (3)	Θ [°] (4)	q [%] (5)	u [%] (6)	Telescope (7)	Filter (8)
60599.227	30	4.12 ± 1.07	-10.3 ± 5.1	3.9 ± 1.0	-1.4 ± 0.8	Skinakas 1.3m	r
60599.250	30	< 4.9	...	-2.3 ± 0.9	0.1 ± 0.6	Skinakas 1.3m	g
60607.226	38	< 13.6	...	1.6 ± 2.4	3.5 ± 3.1	Skinakas 1.3m	r
60710.256	141	$24.4^{+7.8}_{-5.9}$	19.2 ± 7.5	-20.7 ± 7.5	-14.6 ± 6.2	NOT	B
60710.279	141	< 28.6	...	7.5 ± 5.2	8.7 ± 4.8	NOT	V
60825.131	256	< 0.49	...	-0.07 ± 0.15	-0.20 ± 0.15	NOT	V
60825.146	256	< 1.3	...	-0.17 ± 0.25	-0.09 ± 0.25	NOT	B
60825.161	256	< 0.41	...	-0.02 ± 0.12	-0.18 ± 0.12	NOT	R

(1) Modified Julian Date of the observation. (2) Time from peak, assumed $t_{\rm peak} = 60569$ MJD [6]. (3) Measured polarization degree (Π). Upper limits are reported at 3σ. (4) Polarization angle, reported only for detections. (5) Stokes parameter q, with the associated uncertainty. (6) Stokes parameter u, with the associated uncertainty. (7) Telescope used for the observation. (8) Observing filter.

negligible. The host was found to be consistent with weak or negligible polarization: $\Pi < 0.49\%$ in the V band, $\Pi < 1.3\%$ in the B band and $\Pi < 0.41\%$ in the R band, all at 3σ confidence. These measurements support the assumption that host-galaxy light mainly dilutes the transient polarization rather than adding a significant polarized component. The host-corrected polarimetric measurements used in this work are listed in Table 1, while the Stokes parameter plot showing the evolution of q and u over time is shown in Figure 2. The only exception is the MJD 60825 host-galaxy sequence, which is not corrected for transient light because the transient had faded and the observations were obtained to characterize the host contribution. Polarization angles are reported only for detections with significance greater than 3σ, because the angle is undetermined in the case of non-detections ($\Pi - 3\sigma_\Pi < 0\%$).

Host galaxy correction

Most optically discovered TDEs occur in nearby galaxies whose stellar light contributes significantly to the measured flux [63]. This is especially important for AT2024tvd because the transient is projected close to extended host-galaxy emission. If the host galaxy is weakly polarized, its main effect is to dilute the polarization of the transient: the observed polarization is lower than the intrinsic polarization because unpolarized stellar light is added to the polarized transient light [40, 44, 46, 47]. Correcting for this dilution is therefore essential. Depending on the dataset we were considering, we employed one of two techniques to correct for host galaxy dilution. For the NOT observations, we modeled and subtracted the host galaxy directly in the polarimetric images. Each ALFOSC polarimetric exposure contains an ordinary and an extraordinary beam (see Figure 3). We fitted the host-galaxy light distribution in both beams with a Sérsic profile [64, 65], convolved with a PSF derived from a bright star in the same field and close to the transient position (see Figure 3 for an exemplary image describing the NOT field of AT2024tvd). The purpose of using a nearby PSF star

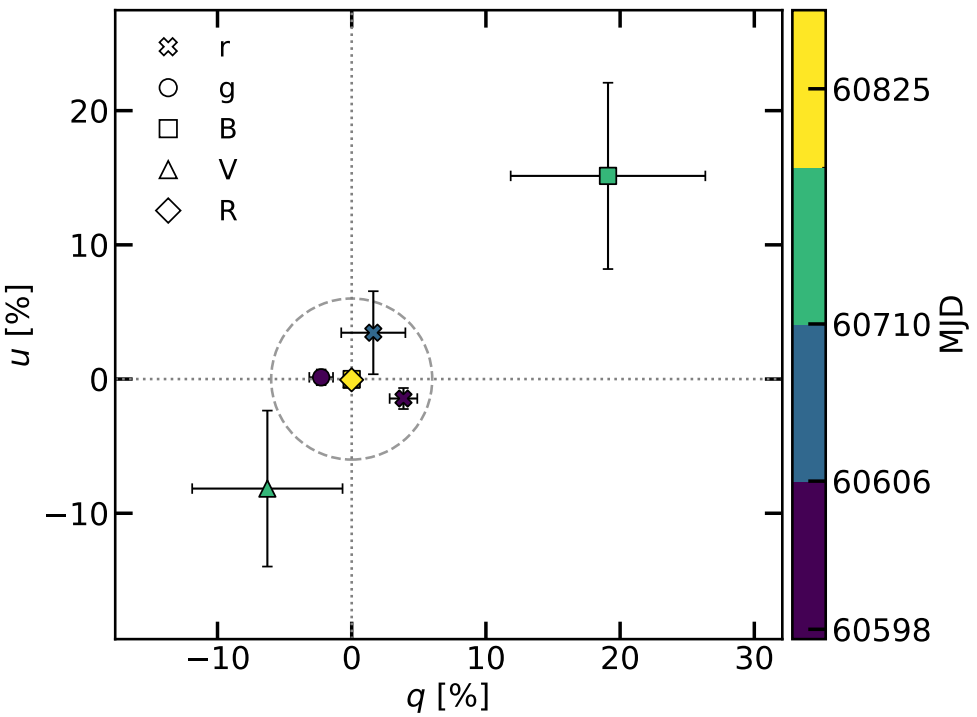


Fig. 2 Stokes q and u parameters for the observations of AT2024tvd. The dashed gray circle marks $\Pi = 6\%$, representative of the level expected from a moderately polarized thermal component [39]. Each observation is color-coded by MJD. The NOT B-band detection lies well outside this region, showing that an additional highly polarized component is required.

was to minimize systematic differences in the image quality across the detector. The Sérsic model and the PSF component were fitted simultaneously at each half-wave plate angle, and the best-fitting host model was subtracted from each image before measuring the Stokes parameters of the transient. This procedure follows the approach used in previous TDE host-subtraction analyses [47]. Figure 4 displays the absence of residuals after removing the host galaxy model. We checked the reliability of the host subtraction in two ways. First, the Sérsic parameters obtained from the polarimetric images are consistent with those obtained from deeper NOT images of the galaxy taken when the transient had faded (the best-fitted host galaxy parameters for each band are shown in Table 2). Second, we measured the polarization of the field star used to construct the PSF. The star is consistent with negligible polarization, with 3σ limits of $\Pi < 0.35\%$ in the V band and $\Pi < 0.64\%$ in the B band. These limits are much smaller than the uncertainty on the transient polarization, and show that the PSF modeling does not introduce a spurious signal comparable to the measured B-band polarization. For the RoboPol observations, direct modeling of the extended host galaxy was not possible because RoboPol is optimized for point-source polarimetry and the extended host structure has low signal-to-noise ratio in the relevant apertures.

We therefore used an aperture-based dilution correction, following the method applied to AT2020mot [40]. We estimated the host-galaxy flux, $I_{\rm host}$, within the same aperture used for the polarization measurement. We then measured the total flux, I, which contains both the host and the transient. Assuming the host light is unpolarized, the intrinsic transient polarization is

$$\Pi_{\rm corr} = \Pi_{\rm obs} \frac{I}{I - I_{\rm host}}, \tag{1}$$

where $\Pi_{\rm obs}$ is the measured polarization before dilution correction. Under the same assumption, the polarization angle Θ is unchanged by the correction, because adding unpolarized light changes the polarization amplitude but not the direction in Stokes space [40, 46, 62]. We derived the host-galaxy fluxes from pre-TDE Pan-STARRS magnitudes [66], and subtracted them in the employed filter using filter transformations from Tonry et al. [67]. The transient flux was either determined from contemporary ZTF photometry in the g- and r- bands or, in the case of the observations with the NOT, directly from the polarimetric images, calibrating the zero-point with standard stars in the field. The measured magnitude of the TDE at the epoch of MJD 60710 is 19.37 ± 0.04 mag and 19.18 ± 0.04 mag in the B- and V-bands, respectively. Additionally, we estimated the maximum galactic interstellar polarization contribution to the observed polarization in the various adopted bands using the Serkowski et al. 68 law and the interstellar extinction extracted from the Schlafly and Finkbeiner 69 reddening maps. Since AT2024tvd lies along a sightline of negligible extinction, this calculation yielded maximum interstellar polarization $\Pi_{\rm max,B} = 0.37\%$, $\Pi_{\rm max,V} = 0.39\%$ and $\Pi_{\rm max,R} = 0.38\%$ in the B,V and R bands, respectively. This result is negligible with respect to the host-corrected polarization of the source, and broadly contained inside the measured upper limits of polarization from the host galaxy.

Table 2 Host galaxy parameters

Band	$\rm Mag_{tot}$ [mag]	$r_{\rm e}$ [kpc]	e	PA [°]	n
(1)	(2)	(3)	(4)	(5)	(6)
B	16.1	1.6	0.45	−40	6.8
V	15.1	1.6	0.45	−36	7.5
R	14.5	1.8	0.45	−34	8.4

(1) Observing band. (2) Total magnitude of the fitted host-galaxy model. (3) Effective radius. (4) Ellipticity. (5) Position angle of the host-galaxy model. (6) Sérsic index.

Multiwavelength observations and X-ray analysis

We compiled optical, radio and X-ray observations in order to compare the polarimetric evolution with the broader evolution of the event. The g-band and optical light curve shown in Fig. 1 was obtained from ZTF data through ALeRCE [22, 70]. The

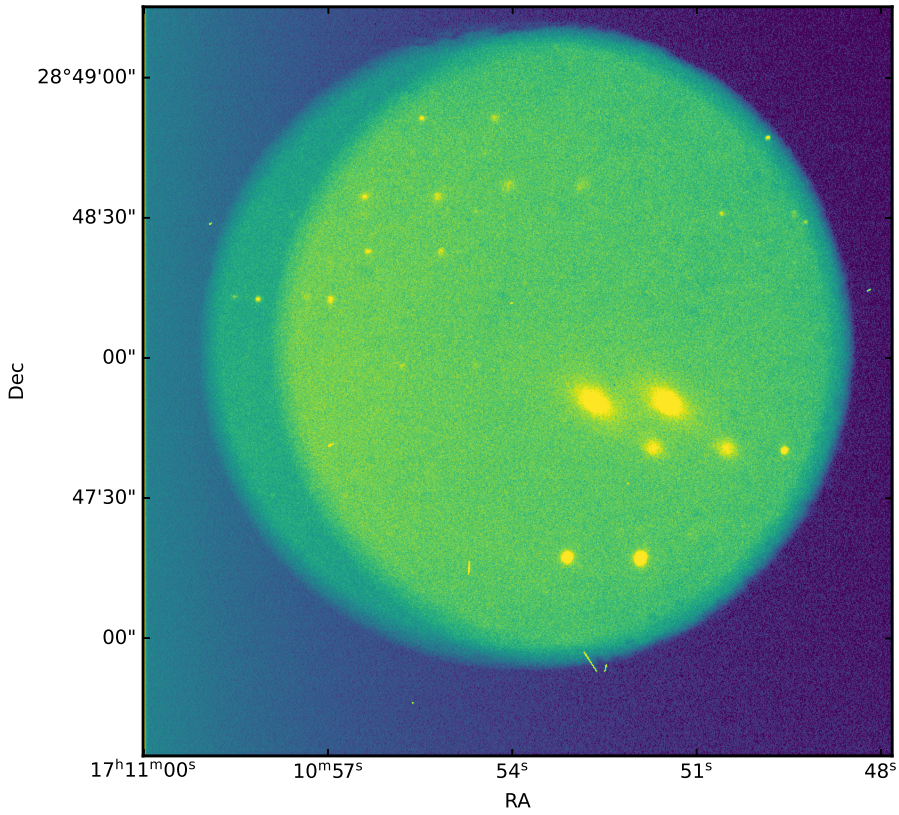


Fig. 3 Example B-band image of the AT2024tvd field obtained with the NOT, with the polarimeter at a position angle of 67.5°. Each source is split into two images corresponding to the extraordinary (left) and ordinary (right) beams. The host galaxy of AT2024tvd is the extended source on the right-hand side of the image. The bright point source in the lower-right corner is the star used to extract the PSF.

radio measurements, including the two radio flares, were published by Sfaradi et al. [8] and accessed through the Open mulTiwavelength Transient Event Repository [60]. The X-ray light curve was constructed from Swift/XRT observations [71].

We constructed the Swift/XRT light curve of AT2024tvd on a per-pointing basis and extracted spectra using `swifttools v3.0` [72] and `HEASOFT v6.35.2`. All observations were obtained in photon-counting (PC) mode. We performed spectral fitting with the Interactive Spectral Interpretation System (ISIS; Houck 73) on the time-averaged spectrum spanning MJD 60593.22–61064.744. The spectrum was grouped to a minimum signal-to-noise ratio (S/N) of 10 below 7.0 keV and to S/N = 5 at higher energies. We converted the 0.3–10 keV count rate to unabsorbed X-ray flux (erg s^{-1} cm^{-2}) using the best-fit model to the averaged spectrum, `tbabs*zashift(bbody+powerlaw)` and fixing the redshift to $z = 0.045$. The best-fit parameters are $N_{\rm H} = 3.9 \times 10^{20}$ cm^{-2} for the equivalent neutral hydrogen column

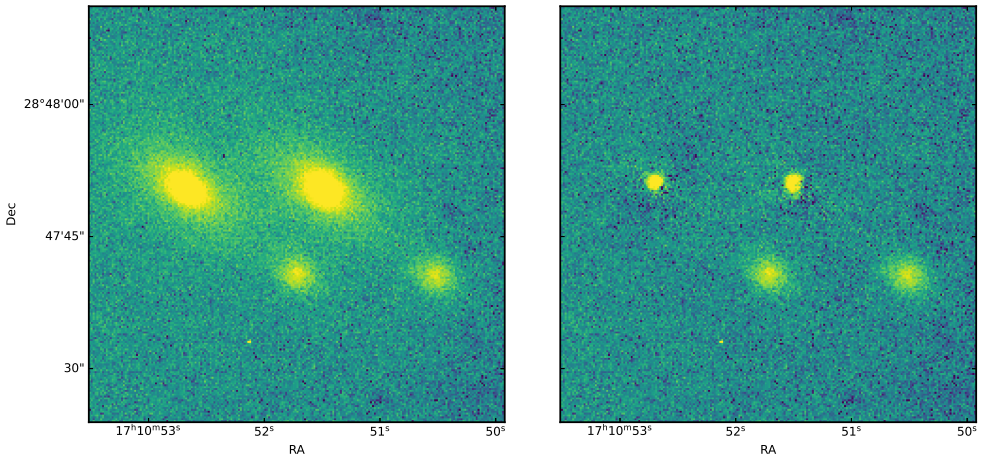


Fig. 4 *Left panel:* Cutout of the sky-subtracted NOT image of AT2024tvd in the B-band, with the polarimeter at a position angle of 67.5°. *Right panel:* Same, but after the host galaxy model was subtracted from the original image, leaving only the TDE.

density, $kT_{\rm bb} = 0.11$ keV for the black body temperature and photon index $\Gamma = 2.6$, yielding $\chi^2/{\rm d.o.f.} = 44.66/52 = 0.86$. We assumed elemental abundances from Wilms et al. [74]. The resulting X-ray light curve is shown in Figure 1.

Estimate of the minimum jet contribution to optical emission

We estimated the minimum contribution of a polarized non-thermal component to the host-subtracted optical emission using the intrinsic B-band polarization measured close to the peak of the X-ray emission. We modeled the host-corrected transient flux as the sum of a thermal component, $F_{\nu,\rm th}$, and a synchrotron component associated with the jet, $F_{\nu,\rm jet}$:

$$F_{\nu,\rm tot} = F_{\nu,\rm th} + F_{\nu,\rm jet}. \tag{2}$$

We define the jet flux fraction as

$$f_{\rm jet} = \frac{F_{\nu,\rm jet}}{F_{\nu,\rm tot}}. \tag{3}$$

If the synchrotron component has intrinsic polarization degree $\Pi_{\rm jet}$ and the thermal component has polarization degree $\Pi_{\rm th}$, then, in the most conservative case in which the two polarization angles are aligned, the observed polarization satisfies

$$\Pi_{\rm obs} = f_{\rm jet}\Pi_{\rm jet} + (1 - f_{\rm jet})\Pi_{\rm th}. \tag{4}$$

Solving for the synchrotron fraction gives

$$f_{\rm jet} = \frac{\Pi_{\rm obs} - \Pi_{\rm th}}{\Pi_{\rm jet} - \Pi_{\rm th}}. \tag{5}$$

This expression provides a lower limit on $f_{\rm jet}$, because any misalignment between the polarization angles of the two components, or any disorder in the magnetic field of the synchrotron-emitting region, would reduce the net observed polarization and therefore require a larger synchrotron contribution.

We adopted the host-corrected B-band polarization $\Pi_{\rm obs} = 24.4^{+7.8}_{-5.9}\%$ and propagated its uncertainty with a Monte Carlo calculation. In each realization, a value of $\Pi_{\rm obs}$ was drawn from a split-normal distribution using the asymmetric lower and upper uncertainties, and the corresponding $f_{\rm jet}$ was computed for a grid of assumed $\Pi_{\rm jet}$ values. The 16th, 50th and 84th percentiles of the resulting $f_{\rm jet}$ distribution were then used to define the median estimate and its 1σ confidence interval, respectively.

For a maximally polarized optically thin synchrotron component, we adopted $\Pi_{\rm jet} = 70\%$. If the thermal component is assumed to be unpolarized, the measured B-band polarization then requires $f_{\rm jet} \gtrsim 0.35^{+0.11}_{-0.08}$. Even in a more conservative case in which the thermal component is allowed to contribute up to $\Pi_{\rm th} = 6\%$ polarization [39] and is assumed to be aligned with the synchrotron component, the required synchrotron fraction remains $f_{\rm jet} \gtrsim 0.29^{+0.12}_{-0.09}$. The results of this calculation are described in Figure 5. Thus, at least about one third of the host-subtracted B-band emission at this epoch must arise from a highly polarized component under conservative assumptions. Lower intrinsic synchrotron polarization, partial cancellation in Stokes space, or magnetic field disorders would all increase the required non-thermal contribution.

Jet evolution and characteristics

We interpret the radio, X-ray and polarization evolution of AT2024tvd using the delayed jet-breakout framework developed for misaligned TDE disks [41]. In a TDE, the fallback rate is initially expected to scale approximately as $\dot{M} \propto t^{-5/3}$ after the most bound debris returns, although real events can deviate from this idealized behavior [2, 14]. If a fraction η of the accreted rest-mass energy is converted into jet power, the jet luminosity can be written as

$$L_{\rm j}(t) \simeq \eta \dot{M}(t) c^2. \tag{6}$$

At early times, the accretion flow is expected to be geometrically thick and to drive a dense disk wind in the super-Eddington regime [4, 12, 13, 15]. If the disk and jet are misaligned with respect to the SMBH spin, Lense–Thirring precession causes the jet direction to sweep through a large angle [41, 75]. This makes it harder for the jet to drill a stable channel through the wind. Teboul and Metzger 41 showed that the critical jet efficiency required for breakout is increased by a factor of order

$$\frac{\psi^2}{\theta_{\rm j}^2}\left(1 + 4\pi^2 \tan^2\psi\right), \tag{7}$$

relative to the non-precessing case, where ψ is the initial misalignment angle and $\theta_{\rm j}$ is the jet half-opening angle [41]. In this framework, moderately powered jets can be hidden at early times and escape only after the disk–jet system aligns with the SMBH spin [41].We associate the first delayed radio flare of AT2024tvd with this delayed escape. The onset of the first radio peak occurs at $\Delta t \simeq$ 88–131 days after optical discovery, and this phase overlaps with the X-ray brightening and hardening reported

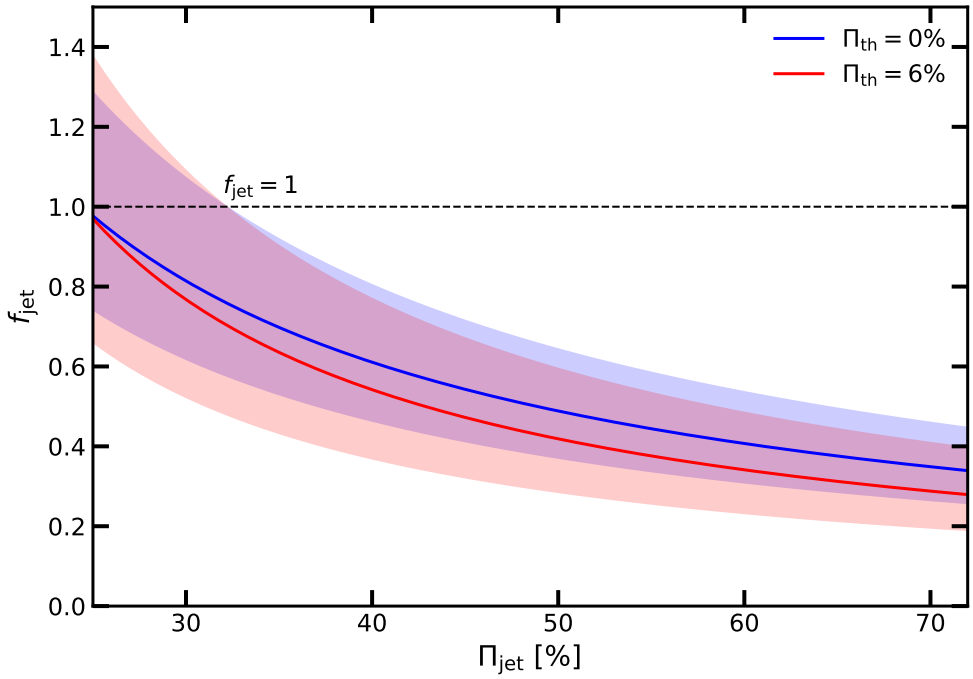


Fig. 5 Minimum synchrotron contribution implied by the host-corrected B-band polarization. The required synchrotron flux fraction, $f_{\rm jet}$, is shown as a function of the assumed intrinsic synchrotron polarization, $\Pi_{\rm jet}$. Curves correspond to different assumptions for the polarization of the thermal component, $\Pi_{\rm th}$. Shaded regions show the 68% interval obtained by propagating the asymmetric uncertainty on the measured polarization.

for the event [6, 8]. We therefore adopt an alignment time of order $t_{\rm align} \sim 80$ days. In the hydrodynamical alignment regime of Teboul and Metzger [41], the alignment time for an expanding disk can be estimated as

$$t_{\rm align} = \left(\frac{10 R_{\rm g}}{\alpha R_{\rm c}} t_{\nu,c}^{2/3} t_{\rm Edd}^{5/3} \right)^{3/7} , \tag{8}$$

where $R_{\rm g} = GM_{\rm BH}/c^2$ is the gravitational radius, α is the Shakura–Sunyaev viscosity parameter, $R_{\rm c}$ is the circularization radius, $t_{\nu,c}$ is the viscous time at $R_{\rm c}$ and $t_{\rm Edd}$ is the time at which the fallback rate becomes Eddington [41]. For a $10^6 M_\odot$ black hole, a solar-mass star and an expanding disk with outer radius $R_{\rm d} = R_{\rm c}(t/t_{\nu,c})^{\chi}$ with $\chi = 2/3$, an alignment time of order 80 days corresponds to $\alpha \simeq 0.2$. The same framework gives an estimate of the jet energy available after breakout. For a fallback-powered jet, the energy released after alignment is

$$E_{\rm j} = \int_{t_{\rm align}}^{\infty} L_{\rm j}(t) dt \simeq \frac{1}{3} \eta (1 - f_{\rm w}) M_\star c^2 \left(\frac{t_{\rm fb}}{t_{\rm align}} \right)^{2/3} , \tag{9}$$

where $f_{\rm w}$ is the fraction of fallback mass lost in winds, $M_\star$ is the stellar mass and $t_{\rm fb}$ is the fallback time of the most bound debris [41]. For $t_{\rm align} \sim 80$ days, $t_{\rm fb} \sim 41$ days, $M_\star \sim 1 M_\odot$ and $\eta \sim 10^{-3}$–10^{-2}, this gives $E_{\rm j} \sim 3.5 \times 10^{50}$–$3.5 \times 10^{51}$ erg, up to the factor $(1 - f_{\rm w})$. We compare this energy scale with the radio-inferred energy of the first flare. Using the first radio peak at $\Delta t \simeq 131$ days, corresponding to about 51 days after the adopted alignment time, and applying standard synchrotron scalings for an outflow interacting with a wind-like circumnuclear medium [76], we obtain an isotropic-equivalent energy of order $E_{\rm iso} \sim 4.5 \times 10^{50}$ erg for microphysical parameters $\epsilon_{\rm e} = 0.1$ and $\epsilon_{\rm B} = 0.01$. This value is consistent, at order-of-magnitude level, with the jet energy expected for a delayed breakout after hydrodynamical alignment. A precessing and aligning jet can also produce a structured angular outflow. Before alignment, the jet deposits energy over a wide angle comparable to the initial misalignment angle ψ. After alignment, the narrow core with half-opening angle $\theta_{\rm j}$ can emerge more directly [41]. In our interpretation, the wide-angle component produces the first delayed radio peak and the associated X-ray hardening, while the narrow core produces the late high-polarization component. The high B-band polarization at $\Delta t \sim 190$ days is nearly contemporaneous with the radio rebrightening at $\Delta t \sim 194$ days [8]. We therefore attribute both signatures to the narrow energetic core of the two-component jet. This interpretation explains why the polarization is modest near optical maximum, when the thermal component dominates, and high only at later times, when the non-thermal core contribution becomes a larger fraction of the observed optical light.